CORE
Metadata, citation and similar papers at core.ac.uk
Provided by Elsevier - Publisher Connector

FEBS Letters 587 (2013) 3412–3416

ELSEVIER

FEBS Letters

journal homepage: www.FEBSLetters.org

Structure of the Toll/interleukin 1 receptor (TIR) domain of the immunosuppressive *Brucella* effector BtpA/Btp1/TcpB

Burcu Kaplan-Türköz [a], Thomas Koelblen [a], Christine Felix [b,c], Marie-Pierre Candusso [a], David O'Callaghan [b,c], Annette C. Vergunst [b,c], Laurent Terradot [a,*]

[a] UMR 5086, BMSSI, CNRS – Université Lyon 1, Institut de Biologie et Chimie des Protéines, 7 passage du Vercors, F-69367, France
[b] INSERM, U1047, UFR Médecine, 186 Chemin du Carreau de Lanes, 30908 Nîmes, Cedex 02, France
[c] Université de Montpellier 1, UFR Médecine, 186 Chemin du Carreau de Lanes, 30908 Nîmes, Cedex 02, France

ARTICLE INFO

Article history:
Received 5 August 2013
Revised 30 August 2013
Accepted 3 September 2013
Available online 25 September 2013

Edited by Renee Tsolis

Keywords:
BtpA
TLR
X-ray crystallography
TIR domain
Structural mimicry
Brucella

ABSTRACT

BtpA/Btp1/TcpB is a virulence factor produced by *Brucella* species that possesses a Toll interleukin-1 receptor (TIR) domain. Once delivered into the host cell, BtpA interacts with MyD88 to interfere with TLR signalling and modulates microtubule dynamics. Here the crystal structure of the BtpA TIR domain at 3.15 Å is presented. The structure shows a dimeric arrangement of a canonical TIR domain, similar to the *Paracoccus denitrificans* Tir protein but secured by a unique long N-terminal α-tail that packs against the TIR:TIR dimer. Structure-based mutations and multi-angle light scattering experiments characterized the BtpA dimer conformation in solution. The structure of BtpA will help with studies to understand the mechanisms involved in its interactions with MyD88 and with microtubules.

Structured digital abstract:
BtpA and **BtpA** bind by x-ray crystallography (View interaction)

© 2013 Federation of European Biochemical Societies. Published by Elsevier B.V. All rights reserved.

1. Introduction

Toll/like receptors (TLRs) are transmembrane proteins that sense pathogens and initiate innate immune signalling cascades. Signalling through TLRs involves homo and heterotypic interactions of their Toll/interleukin 1 receptor (TIR) domains with cytosolic TIR domain containing adaptors such as MyD88 and TIRAP, that leads to proinflammatory responses [1]. Structural studies have revealed that TIR domains consist of a parallel five-stranded β sheet (βA–βE) surrounded by α helices (αA–αE) connected by more variable loops, probably illustrating the versatile nature of these domains [2–10].

Because of their central role in host defence, TLR signalling pathways are targets for bacterial pathogens to modulate host innate immune responses during the course of infection. One recently discovered strategy involves bacterial TIR domain-containing proteins of pathogenic bacteria that interfere directly with TLR signalling [11]. The bacterial TIR proteins TcpC (*Escherichia coli*), TcpB/Btp1 (*Brucella*), TlpA (*Salmonella enterica*) and YpdTir (*Yersinia pestis*) have been studied in detail [12–15].

The zoonotic pathogen *Brucella* is the causative agent of brucellosis (or Malta fever) and relies on its VirB type IV secretion system (T4SS) to survive and multiply within host-cells [16–18]. *Brucella* species produce a TIR protein named BtpA (previously called Btp1 or TcpB [12,13]) translocated by the *Brucella* T4SS into host cells during infection [13,14,19]. Here, BtpA interferes with TLR2 and TLR4 signalling, resulting in the reduction of dendritic cell (DC) maturation, inhibition of pro-inflammatory cytokine secretion [13] and impaired NF-κB activation in macrophages [14], possibly by inducing the ubiquitination and degradation of TIRAP [20]. In vivo pull down assays showed that BtpA interacts with TIRAP but not with MyD88 [20]. However yeast two-hybrid assays established that BtpA interacts with MyD88 [21]. Moreover, in vivo split-GFP experiments showed that the interaction with BtpA requires the MyD88 death domain, rather than the TIR domain [21]. The BtpA TIR domain, however, has been shown to be required for association with microtubules, and to prevent microtubule depolymerisation [22].

To better understand the structural basis of the mode of action of BtpA we have solved the crystal structure of its TIR domain at 3.15 Å. The structure shows a canonical TIR fold and a quaternary arrangement resembling that of the *Paracoccus denitrificans* TIR domain (PdTIR) [5]. Our structural and biochemical characterisation

* Corresponding author. Fax: +33 4 72 72 26 04.
E-mail address: laurent.terradot@ibcp.fr (L. Terradot).

0014-5793/$36.00 © 2013 Federation of European Biochemical Societies. Published by Elsevier B.V. All rights reserved.
http://dx.doi.org/10.1016/j.febslet.2013.09.007

of the protein defines the structure of the BtpA dimer, which has important implications for its mode of action in the host cell.

2. Materials and methods

2.1. Cloning, expression, and purification of BtpA

A 828 bp PCR fragment encoding BtpA from *Brucella melitensis* 16M genomic DNA was cloned into the pET151D topo vector (Invitrogen). Point mutations were introduced using the QuickChange mutagenesis kit (Stratagene) following manufacturer's protocol. *E. coli* BL21(DE3) cells carrying the resulting plasmids were grown in LB media containing ampicillin at 37 °C until an OD_{600} of 0.7 when protein expression was induced by the addition of 1 mM isopropyl-β-D-thiogalactopyranoside overnight at 20 °C. Harvested cells were resuspended in lysis buffer (40 mM Tris pH 8, 300 mM NaCl, 10% (v/v) glycerol, 1% (v/v) Triton X-100) supplemented with Dnase-I, lysozyme, and protease inhibitor tablets (Roche). After sonication the cell lysate was cleared by centrifugation (16000*g* for 20 min). The cell lysate was loaded onto a 5-ml His-Trap column (GE Healthcare) pre-equilibrated with buffer A (40 mM Tris pH 8, 250 mM NaCl, 5% (v/v) glycerol). The column was washed successively with buffer A, 10% (v/v) buffer B (buffer A with 500 mM imidazole), and 1 M NaCl. The protein was eluted with a linear gradient from 10–100% of buffer B. The fractions containing 6his-BtpA containing were pooled and frozen. Protein used for crystallogenesis was incubated with TEV protease (1:40), 1 mM DTT and 0.5 mM EDTA, dialysed against buffer A at 4 °C overnight and then loaded on a His-trap column. Pure BtpA eluted with 10% (v/v) buffer B. BtpA and 6his-BtpA were concentrated to 10 mg/ml and applied to size exclusion chromatography (Superdex 75; GE Healthcare) in buffer A. Similar protocols were used for production of BtpA variants except that the 6his-tag was not cleaved.

2.2. Multi angle laser light scattering

Size-exclusion chromatography combined with multi angle laser light scattering (MALLS) and refractometry experiments were performed with an analytical Superdex 75 column (GE Healthcare) equilibrated with buffer A. On-line MALLS detection was performed with a miniDAWN-TREOS detector (Wyatt Technology) using a laser emitting at 690 nm and by refractive index measurement using an Optilab T-rex system (Wyatt Technology). Weight averaged molar masses (Mw) were calculated using the ASTRA software (Wyatt Technology).

2.3. Crystallisation, structure determination, and refinement

BtpA crystals were obtained using the vapor-diffusion methods by mixing 1.0 µl of protein with 1.0 µl of reservoir solution containing PEG 4000 23–30%, (v/v), 100 mM sodium citrate pH 5.4–5.6 and 200 mM ammonium acetate. Crystals were flash-frozen in liquid nitrogen after addition of a cryoprotectant solution consisting of reservoir solution with glycerol (10% v/v). X-ray diffraction data were collected from native crystals at the ID23EH1 beamline of the ESRF (Grenoble). Data were indexed and integrated using XDS [23] and scaled with SCALA [24]. The structure of BtpA was solved by molecular replacement using Phaser [25,26] with the PdTIR structure as a template (PDB 3H16) [5]. Initial molecular replacement was done to search for two copies in the asymmetric unit. The visual inspection of the electron density map identified that the asymmetric unit contained four TIR domains. The molecular replacement was repeated to search for four copies and the model was build using Coot [27] and refined using Phenix [28]. Data collection and refinement statistics are given in Table 1. The coordinates of the BtpA TIR domain structure have been deposited in the PDB, entry code 4LZP.

Table 1
Data collection and refinement statistics.

	BtpA TIR
Space group	$P22_12_1$
Wavelength (Å)	0.97627
Cell parameters, *a*, *b*, *c* (Å)	68.14, 73.93, 137.64
Resolution range (Å)	48.4–3.15 (3.26–3.15)
R_{merge}	0.169 (0.66)
$R_{p.i.m.}$	0.112 (0.47)
Number of observed reflections	43030 (6288)
Number of unique reflections	12251 (1768)
Mean ($I/s(I)$)	5.3 (1.5)
Completeness (%)	98.1 (99.2)
Multiplicity	3.5 (3.6)
Refinement statistics	
Resolution range for refinement (Å)	48.4–3.15
Number of unique reflections in refinement	22751
Working set	21668
Test set	1083
Completeness (%)	97.9
Monomers/ASU	4
No. protein atoms	4669
R_{work}/R_{free}	0.222/0.278
R_{msd} bonds (Å)	0.009
R_{msd} angles (o)	1.0
Ramachandran plot	
Most favoured (%)	94.2
Allowed (%) and generously allowed (%)	5.8
Outliers (%)	0

[a]Values in parentheses refer to the indicated resolution shell.

3. Results

3.1. Structure of the BtpA Tir domain

The structure of BtpA was solved at 3.15 Å and refined to final R_{work}/R_{free} values of 22%/27%. Even though crystallization drops were set-up with full-length BtpA, the crystals only contained a C-terminal portion of the protein due to N-terminal degradation. The asymmetric unit (AU) of BtpA crystals contains four chains arranged as two dimers AB and CD. Chains A and C encompass residues 100 to 275 and chains B and D are composed of residues 143 to 275 with some loops missing. As dimers AB and CD are almost identical, only chains A and B will be described in this section. Residues 100 to 133 of chain A form a long helix hereafter named α-tail, that packs against the TIR domains of chains A and B (Fig. 1A), comprised between residues 143 to 275. The TIR domain of BtpA contains the canonical secondary structures described for TIR domains: five parallel β-strands (βA to βE) surrounded by five α-helices (Fig. 1A). There was no interpretable electron density for the loop between αC and βD (CD loop) and for the loop connecting the α-tail to the TIR domain (Fig. 1A). The TIR domains of the four chains are almost identical and are more similar to the structure of PdTIR than to other TIR domains (Fig. 1B and Fig. S1). Although the structures of PdTIR and BtpA TIR domains are very similar, their DE loops are very different. Instead of a loop in PdTIR, BtpA shows a short hydrophobic helix (D′). Interestingly a similar short helix is present in the Myd88 and TIRAP/MAL adaptor proteins at this position although the remaining parts of the TIR domain of these proteins are different (Fig. 1B).

3.2. A conserved dimeric organization in BtpA and PdTIR

In the asymmetric unit, the four chains present two different interfaces similar to those observed for PdTIR. The most significant

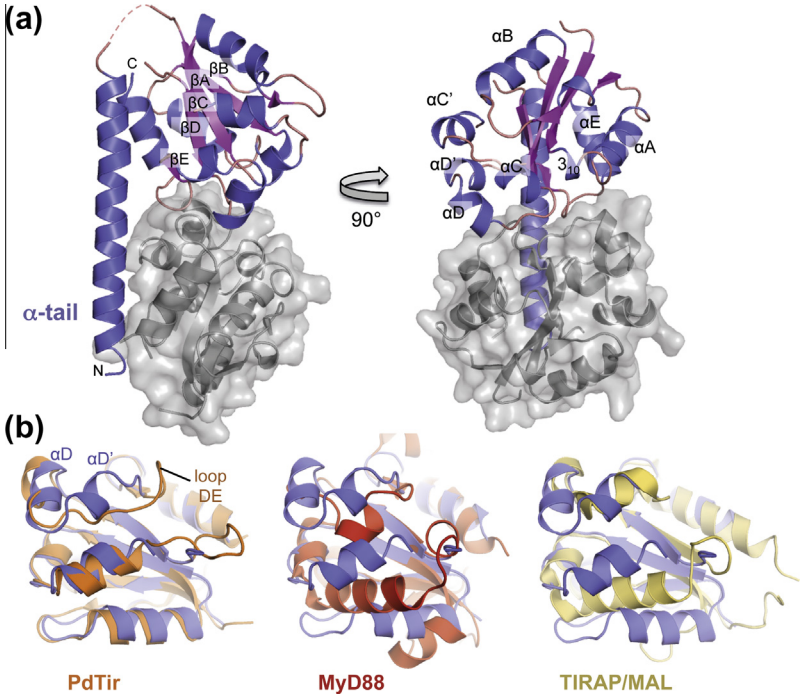

Fig. 1. (A) Two different cartoon representations of the BtpA dimer between chain A and chain B. Chain A is coloured according to secondary structure: helices in blue, strands in magenta and loops in pink. Chain B is coloured in grey with its surface represented in transparency. (B) Structure superimposition of the BtpA TIR domain (blue) with PdTir (orange), MyD88 (red) and TIRAP/MAL (yellow).

interface (I) is found in the dimers AB and CD. A second significant interface (II) involved chain B and chain C (Fig. 2). Additional interfaces were also identified in the crystal packing but rely probably on non-specific interactions as described in other TIR structures [2,5]. Dimers AB and CD are composed of two TIR domains and one α-tail and are almost identical with an interface burying 1200 Å^2. The interface I relies on extensive electrostatic interactions between the DD loop of one chain and EE loop and αC and

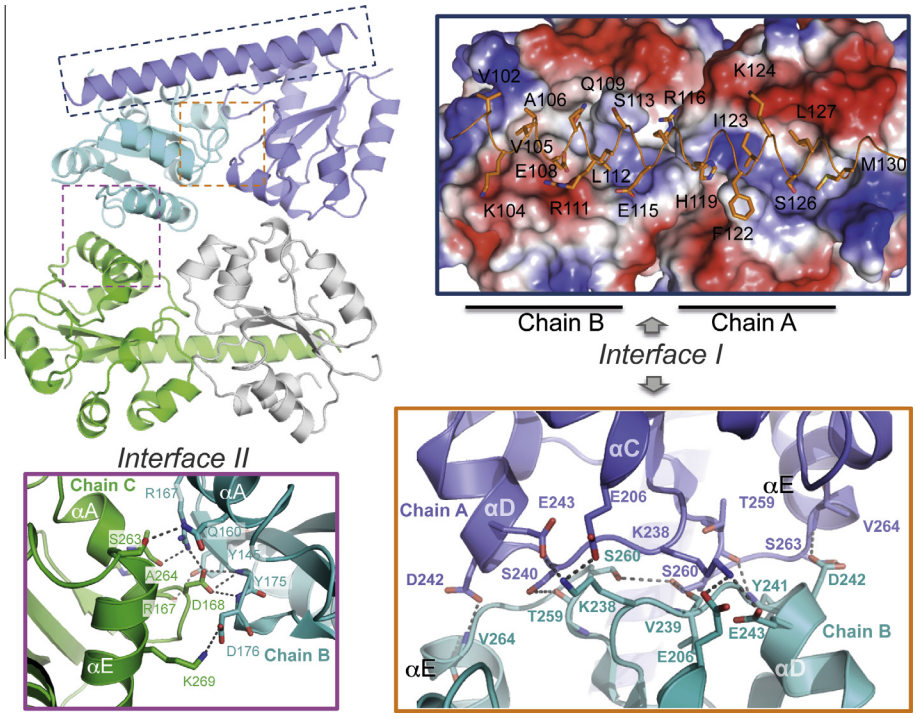

Fig. 2. (A) Ribbon representation of the BtpA crystal asymmetric unit showing chain A (dark blue), B (cyan), C (green) and D (grey) with two close-up views of interface I (blue and orange inserts) and one of interface II (pink insert). The orange insert shows the surface charge representation (blue positive and red negative) of the hydrophobic groove formed by the two TIR monomers. The α-tail is shown in ribbon and coloured in orange. The side chain making contacts with the TIR domains are represented in ball-and-stick and coloured in slate (carbon), red (oxygen), blue (nitrogen) or yellow (sulphur).

αD of the other (Fig. 2). S240 (DD loop) of chain A hydrogen bonds with carbonyl of T259 (EE loop) of chain B. S260 (EE loop) hydroxyl of the two chains formed H-bonds and S260 of chain A also interacts with backbone nitrogen of chain B V239 (DD loop). Reciprocal interaction occurs between the side chain of D242 and of S263 (EE loop) and backbone nitrogen of V264 (αE) and main chain-main chain hydrogen bonds between carbonyl of T259 (EE loop) and nitrogen Y241 (αD). K238 (DD loop) of chain A forms a salt bridge with E206 and E243 (αC and αD, respectively) of chain B and vice versa, an interaction conserved in the PdTIR dimer (K260–E265). In BtpA, the α-tail of chain A packs against both TIR domains of the AB dimer and inserts into a hydrophobic groove formed by the two TIR domains (Fig. 2). In addition to the numerous hydrophobic interactions mediated by side chains from the α-tail residues, several hydrogen bonds secure the position of the helix (Fig. 2). It is noteworthy that in this conformation, the α-tail of only one subunit can be accommodated into the groove since the dimer is symmetrical. So although the TIR:TIR dimer is symmetric, this organisation suggests an asymmetric position for the coiled–coiled domain of BtpA.

The interface II was found between chains B and C and involved amino acids from αA, BB loop, αE and EE loop. The interface also relies on electrostatic interaction, including salt bridges between chain B K269 (αE) and chain C D176 (BB loop), and chain B D168 (αA) and chain C R167 (αA). H-bonds were present between chain B and C residues; S263 (EE) with Q160 (αA), backbone oxygen of A164 (αA) with side chain of R167 (αA), backbone oxygen of R167 with side chain of Y144 (βA) and D168 with backbone nitrogen atoms of Y175 (BB) and D176 (BB). The interface II had an area of 295 Å^2.

3.3. Mutational and biochemical characterisation of the BtpA dimer

To confirm that the dimer was mediated via interface I, we generated BtpA variants aiming to disrupt interface I (S260A, K238E, K238A, K238AS20A) or interface II (R167E, D176R) (Fig. S1). The proteins were purified and their oligomeric states were evaluated by size exclusion chromatography coupled (SEC) to multi angle laser light scattering (MALLS) (Table 2). The purified BtpA with the His-tag has a molecular mass of 34.7 kDa. The elution volume of the protein in SEC is 9.1 ml and the calculated mass is 68 kDa. These values indicate that BtpA is a dimer in solution. For the variants K238E and K238A, the proteins were hardly expressed in *E. coli* suggesting that these changes affected protein stability and/or were toxic for *E. coli*. Soluble BtpA variant proteins could be obtained for S260A, R167E, D176R and, to a lesser extent, for K238AS260A (Table 2). SEC-MALLS experiments showed that the molecular mass obtained for S260A was 56 kDa with an elution volume of 10.1 ml. A similar elution volume was obtained for the K238AS260A protein but the molecular mass could not be estimated (Table 2). In contrast, variants targeting interface II showed similar elution volumes and molecular masses to wild type BtpA (Table 2). These data suggest that the stability of the dimer was affected, although not disrupted, by changing the DD–EE loop contacts at interface I. Disrupting the DD–EE loop interface was not sufficient to abolish dimer formation: this could be due to the stabilizing effect of the α-tail wrapping of the TIR domains. Changing residues from interface II had no effect on the protein stability or oligomeric state. The AB dimer (interface I) is therefore more likely to represent the conformation of the protein in solution, a conformation in agreement with the study of the dimeric PdTIR where this interface was assessed by deuterium exchange experiments [5].

Table 2
Biochemical characterisation of His-BtpA and His-BtpA protein variants.

BtpA	Interface/structural element	Yield[a]	Elution volume (ml)	MM[b] (kDa)
WT		+++	9.1	68 (1%)
S260A	I/EE loop	++	10.1	56 (4%)
K238E	I/DD loop	–		
K238A	I/DD loop	–		
K238ES260A	I/	+	10.1	ND
R167E	II/αA	+++	9.1	67.7 (2%)
D176R	II/βB	+++	9.1	81.4 (5%)

[a] Yields range from no soluble protein (–) to 2 mg of purified protein/litre of *E. coli* cell culture (+++).
[b] MM: molecular mass obtained in multi angle laser light scattering experiments. Values in parentheses indicate the corresponding error percentage estimated with the ASTRA software.

4. Discussion

TIR domain proteins from pathogenic bacteria have recently emerged as a new class of virulence proteins directly targeting TLR-dependent immune signalling [11,13,14]. Two translocated *Brucella* effector proteins, BtpA and BtpB [19] were identified as TIR domain-containing proteins, but their mode(s) of action is still poorly understood. The only bacterial TIR protein that has been crystallized so far is PdTIR from non-pathogenic *P. denitrificans* [5]. The structure of the *Brucella* BtpA TIR domain we have solved shows most resemblance to PdTIR except for the DE loop that is more similar to those of mammalian MyD88 and TIRAP. The structures of PdTIR and BtpA dimers are very similar. This dimer architecture raises important functional questions about TIR-containing bacterial virulence factors. Indeed, a peptide derived from TcpC DD loop was found to bind to the MyD88 TIR domain [2]. The organisation of the dimer as seen in the crystal structure of BtpA buries most of the DD loop residues side chains making it unlikely that BtpA interacts with MyD88 via the same residues as TcpC (Fig. 3). Accordingly BtpA was found to bind the MyD88 death domain [21]. These elements suggest that TcpC and BtpA, despite sharing a TIR domain, are likely to have different modes of binding to MyD88 and thus most likely play different roles during infection.

Our BtpA structure revealed that a unique α-tail wraps around two TIR domains hereby delineating a large hydrophobic groove formed by the dimer. This original organisation is observed for the first time in TIR domain interactions and reinforces the hypothesis that the AB dimer is physiologically relevant. It suggests that the full length BtpA dimer is not symmetrical and that N-terminal domains might interact with each other independently to form a separate functional unit. However, considering that the loop connecting the α-tail to the TIR domain appears very flexible, different organisations of the full-length protein dimer might also be possible in solution since the N-terminus is believed to form coiled-coils [29].

In addition to a role in inhibition of TLR signalling, BtpA was shown to modify microtubule dynamics [22,30]. The structure reveals that the surface containing the last residues of the BB loop is accessible, in particular, G183 (Fig. 3 and Fig. S1). This residue has been shown to be critical for BtpA interaction with microtubules, as well as inhibition of TLR signalling, and a link between these processes has been hypothesised [22]. The structure of BtpA suggests that in the present conformation, a dimer of BtpA presents two binding sites at opposite sides of the dimer (Fig. 3). Biochemical and structural work to further refine and characterize the structure of BtpA is on-going to be able to address these questions. The presented crystal structure will facilitate future studies aiming at deciphering the molecular details of how BtpA and other

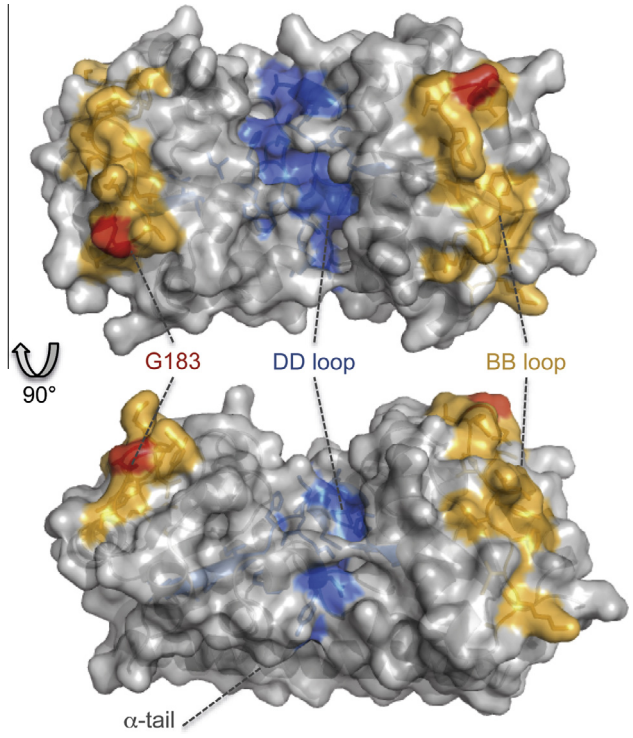

Fig. 3. Two different views of the accessible surface of the BtpA dimer. Residues from the BB loop are coloured in orange, G183 in red and DD loop in blue.

bacterial TIR proteins modulate the innate immune response during bacterial infections, but also help in better understanding the evolutionary basis of TIR proteins, and possible differences between the yet uncharacterized role of non-pathogenic versus pathogenic bacterial TIR proteins.

Acknowledgments

This research was supported by the CNRS ATIP+ program to L.T. and B.K. We thank staff members of ESRF and acknowledge the use of the UMS3444 crystallogenesis and CCMP platforms. Work in INSERM U1047 was supported by grants from the ANR MIME (T4SS) and MIE (BruCell).

Appendix A. Supplementary data

Supplementary data associated with this article can be found, in the online version, at http://dx.doi.org/10.1016/j.febslet.2013.09.007.

References

[1] Akira, S. and Takeda, K. (2004) Toll-like receptor signalling. Nat. Rev. Immunol. 4, 499–511.
[2] Snyder, G.A., Cirl, C., Jiang, J., Chen, K., Waldhuber, A., Smith, P., Rommler, F., Snyder, N., Fresquez, T., Durr, S., et al. (2013) Molecular mechanisms for the subversion of MyD88 signaling by TcpC from virulent uropathogenic *Escherichia coli*. Proc. Natl. Acad. Sci. USA 110, 6985–6990.
[3] Valkov, E., Stamp, A., Dimaio, F., Baker, D., Verstak, B., Roversi, P., Kellie, S., Sweet, M.J., Mansell, A., Gay, N.J., et al. (2011) Crystal structure of Toll-like receptor adaptor MAL/TIRAP reveals the molecular basis for signal transduction and disease protection. Proc. Natl. Acad. Sci. USA 108, 14879–14884.
[4] Chan, S.L., Mukasa, T., Santelli, E., Low, L.Y. and Pascual, J. (2010) The crystal structure of a TIR domain from *Arabidopsis* thaliana reveals a conserved helical region unique to plants. Protein Sci. 19, 155–161.
[5] Chan, S.L., Low, L.Y., Hsu, S., Li, S., Liu, T., Santelli, E., Le Negrate, G., Reed, J.C., Woods Jr., V.L. and Pascual, J. (2009) Molecular mimicry in innate immunity: crystal structure of a bacterial TIR domain. J. Biol. Chem. 284, 21386–21392.
[6] Nyman, T., Stenmark, P., Flodin, S., Johansson, I., Hammarstrom, M. and Nordlund, P. (2008) The crystal structure of the human Toll-like receptor 10 cytoplasmic domain reveals a putative signaling dimer. J. Biol. Chem. 283, 11861–11865.
[7] Choe, J., Kelker, M.S. and Wilson, I.A. (2005) Crystal structure of human Toll-like receptor 3 (TLR3) ectodomain. Science 309, 581–585.
[8] Lin, Z., Lu, J., Zhou, W. and Shen, Y. (2012) Structural insights into TIR domain specificity of the bridging adaptor Mal in TLR4 signaling. PLoS One 7, e34202.
[9] Bernoux, M., Ve, T., Williams, S., Warren, C., Hatters, D., Valkov, E., Zhang, X., Ellis, J.G., Kobe, B. and Dodds, P.N. (2011) Structural and functional analysis of a plant resistance protein TIR domain reveals interfaces for self-association, signaling, and autoregulation. Cell Host Microbe 9, 200–211.
[10] Ohnishi, H., Tochio, H., Kato, Z., Orii, K.E., Li, A., Kimura, T., Hiroaki, H., Kondo, N. and Shirakawa, M. (2009) Structural basis for the multiple interactions of the MyD88 TIR domain in TLR4 signaling. Proc. Natl. Acad. Sci. USA 106, 10260–10265.
[11] Rana, R.R., Zhang, M., Spear, A.M., Atkins, H.S. and Byrne, B. (2013) Bacterial TIR-containing proteins and host innate immune system evasion. Med. Microbiol. Immunol. 202, 1–10.
[12] Rana, R.R., Simpson, P., Zhang, M., Jennions, M., Ukegbu, C., Spear, A.M., Alguel, Y., Matthews, S.J., Atkins, H.S. and Byrne, B. (2011) *Yersinia pestis* TIR-domain protein forms dimers that interact with the human adaptor protein MyD88. Microb. Pathog. 51, 89–95.
[13] Salcedo, S.P., Marchesini, M.I., Lelouard, H., Fugier, E., Jolly, G., Balor, S., Muller, A., Lapaque, N., Demaria, O., Alexopoulou, L., et al. (2008) *Brucella* control of dendritic cell maturation is dependent on the TIR-containing protein Btp1. PLoS Pathog. 4, e21.
[14] Cirl, C., Wieser, A., Yadav, M., Duerr, S., Schubert, S., Fischer, H., Stappert, D., Wantia, N., Rodriguez, N., Wagner, H., et al. (2008) Subversion of Toll-like receptor signaling by a unique family of bacterial Toll/interleukin-1 receptor domain-containing proteins. Nat. Med. 14, 399–406.
[15] Newman, R.M., Salunkhe, P., Godzik, A. and Reed, J.C. (2006) Identification and characterization of a novel bacterial virulence factor that shares homology with mammalian Toll/interleukin-1 receptor family proteins. Infect. Immunol. 74, 594–601.
[16] Lacerda, T.L., Salcedo, S.P. and Gorvel, J.P. (2013) *Brucella* T4SS: the VIP pass inside host cells. Curr. Opin. Microbiol. 16, 45–51.
[17] O'Callaghan, D. and Whatmore, A.M. (2011) *Brucella* genomics as we enter the multi-genome era. Brief Funct. Genomics 10, 334–341.
[18] O'Callaghan, D., Cazevieille, C., Allardet-Servent, A., Boschiroli, M.L., Bourg, G., Foulongne, V., Frutos, P., Kulakov, Y. and Ramuz, M. (1999) A homologue of the *Agrobacterium tumefaciens* VirB and *Bordetella pertussis* Ptl type IV secretion systems is essential for intracellular survival of *Brucella suis*. Mol. Microbiol. 33, 1210–1220.
[19] Salcedo, S.P., Marchesini, M.I., Degos, C., Terwagne, M., Von Bargen, K., Lepidi, H., Herrmann, C.K., Santos Lacerda, T.L., Imbert, P.R., Pierre, P., et al. (2013) BtpB, a novel *Brucella* TIR-containing effector protein with immune modulatory functions. Front. Cell Infect. Microbiol. 3, 28.
[20] Sengupta, D., Koblansky, A., Gaines, J., Brown, T., West, A.P., Zhang, D., Nishikawa, T., Park, S.G., Roop 2nd, R.M. and Ghosh, S. (2010) Subversion of innate immune responses by *Brucella* through the targeted degradation of the TLR signaling adapter. J. Immunol. 184, 956–964.
[21] Chaudhary, A., Ganguly, K., Cabantous, S., Waldo, G.S., Micheva-Viteva, S.N., Nag, K., Hlavacek, W.S. and Tung, C.S. (2012) The *Brucella* TIR-like protein TcpB interacts with the death domain of MyD88. Biochem. Biophys. Res. Commun. 417, 299–304.
[22] Radhakrishnan, G.K., Harms, J.S. and Splitter, G.A. (2011) Modulation of microtubule dynamics by a TIR domain protein from the intracellular pathogen *Brucella melitensis*. Biochem. J. 439, 79–83.
[23] Kabsch, W. (1993) Automatic processing of rotation diffraction data from crystals of initially unknown symmetry and cell constants. J. Appl. Crystallogr. 26, 795–800.
[24] Collaborative Computational Project N (1994) The CCP4 suite: programs for protein crystallography. Acta Crystallogr., Sect. D: Biol. Crystallogr. 50, 760–763.
[25] McCoy, A.J., Grosse-Kunstleve, R.W., Adams, P.D., Winn, M.D., Storoni, L.C. and Read, R.J. (2007) Phaser crystallographic software. J. Appl. Crystallogr. 40, 658–674.
[26] Winn, M.D., Ballard, C.C., Cowtan, K.D., Dodson, E.J., Emsley, P., Evans, P.R., Keegan, R.M., Krissinel, E.B., Leslie, A.G., McCoy, A., et al. (2011) Overview of the CCP4 suite and current developments. Acta Crystallogr., Sect. D: Biol. Crystallogr. 67, 235–242.
[27] Emsley, P. and Cowtan, K. (2004) Coot: model-building tools for molecular graphics. Acta Crystallogr., Sect. D: Biol. Crystallogr. 60, 2126–2132.
[28] Adams, P.D., Grosse-Kunstleve, R.W., Hung, L.W., Ioerger, T.R., McCoy, A.J., Moriarty, N.W., Read, R.J., Sacchettini, J.C., Sauter, N.K. and Terwilliger, T.C. (2002) PHENIX: building new software for automated crystallographic structure determination. Acta Crystallogr., Sect. D: Biol. Crystallogr. 58, 1948–1954. Epub 2002 Oct 1921.
[29] Fekonja, O., Bencina, M. and Jerala, R. (2012) Toll/interleukin-1 receptor domain dimers as the platform for activation and enhanced inhibition of Toll-like receptor signaling. J. Biol. Chem. 287, 30993–31002.
[30] Radhakrishnan, G.K., Yu, Q., Harms, J.S. and Splitter, G.A. (2009) *Brucella* TIR domain-containing protein mimics properties of the Toll-like receptor adaptor protein TIRAP. J. Biol. Chem. 284, 9892–9898.